Original Research Paper

IJES *Iranian Journal of Earth Sciences*
Vol. 15, No. 4, 2023, 219-227.
DOI:10.30495/ijes.2023.1958430.1756

Earthquake ground-motion prediction in the Khalkhal region, NW Iran

AkramAlizadeh[*1], Fatemeh Salehi[1], Ramin Sadeghi[1]

1. Department of Geology, Faculty of Science, Urmia University, Iran.

Received 16 May 2022; accepted 17 November 2022

Abstract

Understanding seismic sources in a region help us to identify the level of ground motion. The area around Khalkhal city in the south of Ardabil province, northwest Iran, is a seismic region that is specially, complex from a geodynamic and tectonic point of view. Prevailing tectonic regimes in different geologic time intervals have caused at least two deformation episodes recorded by faults, folds and other tectonic structures. These structures indicate that the dominant tectonic regimes have been compressive. Examination of the seismic power of currently active faults and software analysis of their focal mechanisms, show that major activity in the region is due to faults with trend north-south and northeast-southwest. The results of this study indicate the seismic capacity of the region and the likely occurrence of earthquakes with a magnitude greater than two on the Richter scale. Also, they show that the probability of earthquakes with magnitudes above 5.3 on the Richter scale is one in one hundred years. High a- and b-values indicate the frequency of earthquakes with low magnitude and the generally high seismicity in the region.

Keywords: *Ground-motion, Seismicity risk, Khalkhal, Talesh, Ardabil*

1. Introduction

The purpose of earthquake studies is to determine the location, magnitude, probability of future earthquake occurrences, and the spatial distribution of their effects. Iran is one of the most seismicity countries in the world and major faults cause destructive earthquake events. The seismotectonic studies is necessary for encountering the hazards of earthquake at any region of Iran. There are two main orogeny, Alborz and Zagros, impact the lithosphere at the north and southwestern Iran. Predicting an earthquake by history of the seismicity of a region help us for planning the civil projects in low risk of damage. Considering the tectonic setting of the Khalkhal area, this research was selected to answer questions about the potential of seismicity in this region.

The Khalkhal region is located in the southern part of Ardabil, to the west of the Alborz Mountains. The Alborz mountain belt extends for several thousand kilometers and is situated between the Caspian Sea and central Iran. It is a part of the Alpine-Himalayan belt that is located between the Eurasian and Cimmerian plates. The extensional phase of the Alpine orogeny caused intense volcanic activity in the Khalkhalregion creating a pyroclastic unit up to 4000m thick (Nazari and Shahidi 2011). There are no radiometric age determinations for the volcanic rocks (Doroozi et al. 2016) but they are associated with BarremianAptian and Cenomanian limestone layers, which clearly indicate that they are Cretaceous (VahdatiDaneshmand and Nadim 2001). Part of the unit contains lavas and pyroclastic rocks with andesite-dacite composition and is interlayered with limestone, marl, and clastic sedimentary rocks. Younger sedimentary and volcanic sequences in the area have Paleocene, Eocene, Oligocene and Miocene ages (Darvishzadeh 2006; Fig 1).

---

*Corresponding author.
*E-mail address (es):*ak.alizadeh@urmia.ac.ir

2. Tectonic Setting

The study area is located in the Alborz-Azerbaijan tectonic zone. A compilation of stratigraphic sections across the south Caspian block indicates three major phases of regional deformation in the early Oligocene, middle Miocene and early Pliocene (Madanipour et al. 2018). The regional convergence direction in the NW margins of the Iranian Plateau changed during the middle Miocene phase of deformation (Madanipour et al. 2018; Dehghan and Yazdi 2023; Karimiazar et al. 2023).Geological studies show that the Khalkhal region can be divided into two blocks: an eastern one consisting of metamorphic and sedimentary rocks of Paleozoic to Late Cretaceous age and a western one consisting of igneous and pyroclastic rocks of Cenozoic age (Fig 1).

There is evidence of two phases of tectonism during the Cenozoic. In the first phase in the late Eocene compressional stress was oriented in a NE-SW direction, whereas during the second phase in the middle Miocene (Sarmatin), compressional stress was oriented in a NW-SE direction. The latter phase caused the evolution of thrust faults with a N-S trend (Sadeghi et al. 2015).

In the Talesh mountain belt at least two major, large-scale, vertical-axis rotations have taken place since the Late Cretaceous: 1) a pre-Eocene 73° ± 17° clockwise rotation and 2) post-Eocene differential rotations. These formed the Z-shaped mountain belt, which lies within a crustal-scale shear zone (Rezaeian et al. 2020). The Khalkhal locality lies in the hinge between the south and middle Talesh mountains, and its declination (48.6°±6.2) indicates a clockwise rotation of approximately 39° since the middle-late Eocene (Rezaeian et al. 2020).

3. Seismicity of the study area

The Earthquake Catalog is one of the most important information resources for assessing the region's tectonics and seismic hazards. In this study, data in the catalog for northwestern Iran have been studied in groups reflecting three time periods: historical earthquakes (the period before 1900 AD), first-generation instrumental earthquakes (1900 to 1963), and second-generation instrumental earthquakes (1963 to 2020). However, we know that many historical and first-generation instrumental earthquakes were not recorded in the catalog, due to the lack of seismic devices, so the catalog entries for these two groups are not complete. The historical and instrumental earthquakes in the catalog for the Khalkhal region are plotted separately in Figure 2.

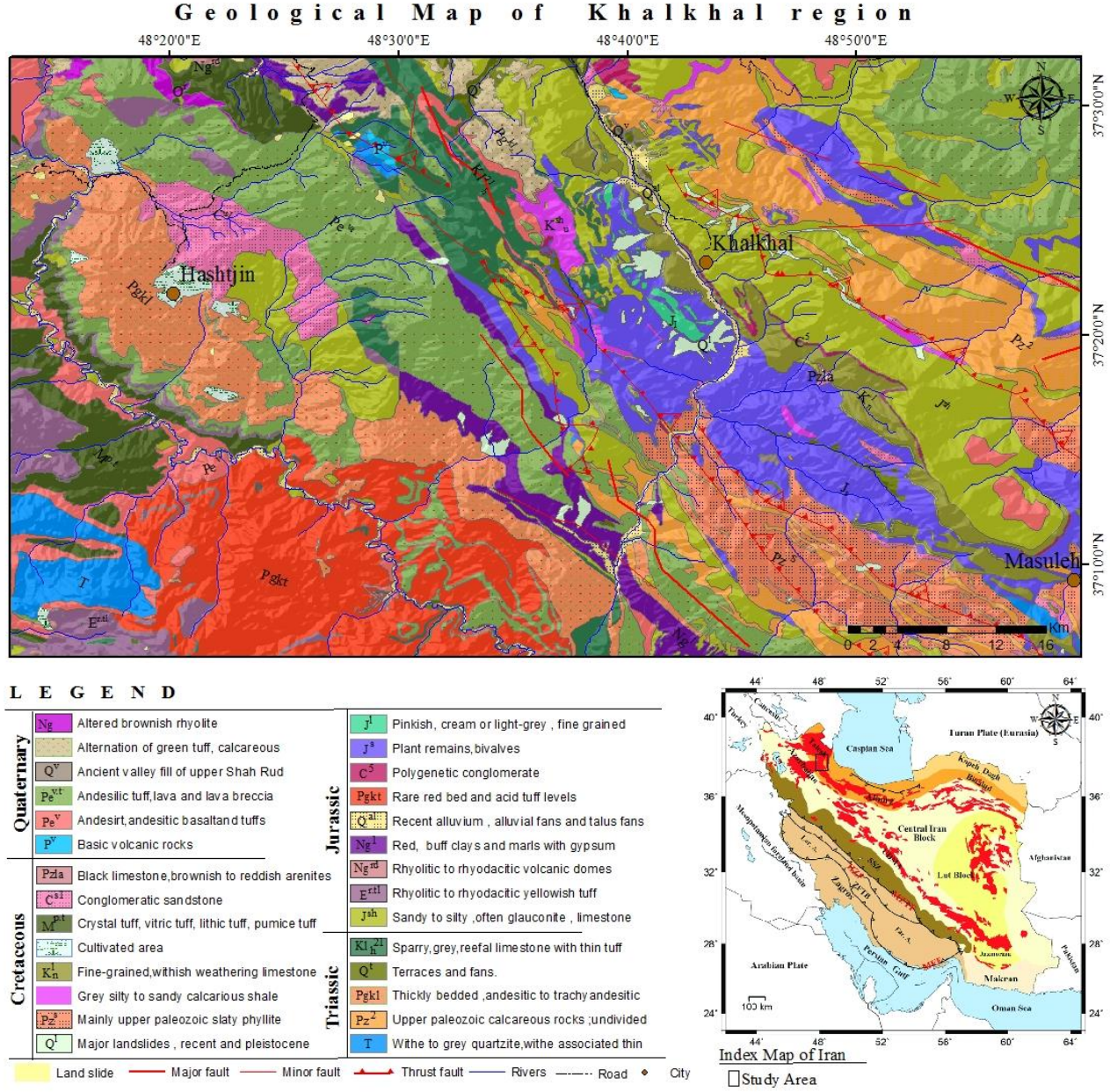

Fig 1. Geological map of the Khalkhal region modified from Asadian et al. (1999).

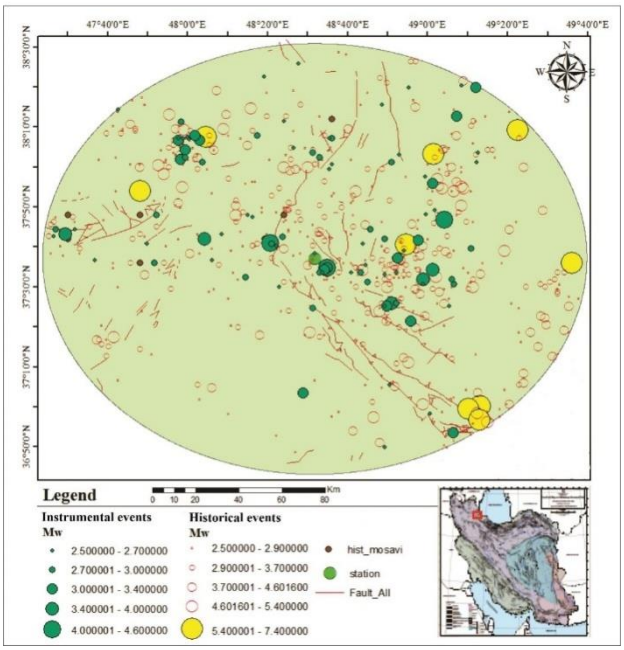

Fig 2. Map of active faults and epicenters of historical and instrumental earthquakes (Ambraseys and Melville 1982) with in 100 km radius of Khalkhal city (at the centre of the map).

Deleting dependent events in the catalog

There are different methods for declustering algorithms for induced seismicity and hazard analysis such as: Gardner and Knopoff (1974); Reasenberg (1985) and the stochastic declustering method (Zhuang et al., 2002). In the present study, the software method of Gardner and Knopoff (1974) has been used, to identify 104 categories of dependent earthquakes, which has resulted in the removal 247 earthquakes from the catalog dataset. The histogram in Figure 3 shows the results obtained from the remaining events after deletion of the dependent events.

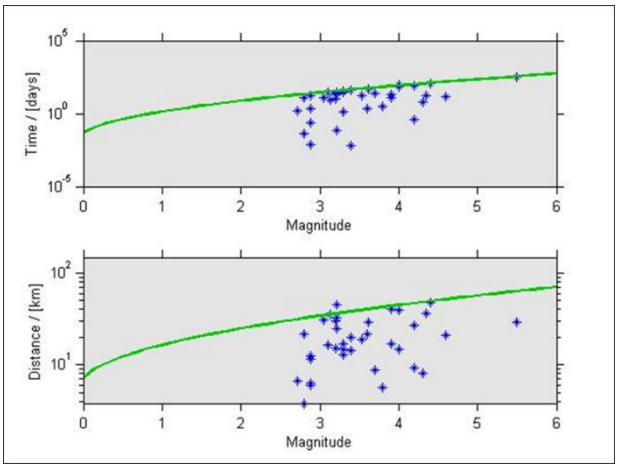

Fig 3. Spatial and temporal window diagram after removing dependent events using Gardner and Knopoff method.

Uncertainties in the size and spatial coordinates of the catalog

The magnitudes of earthquakes are key in determining the seismic parameters and geographical coordinates of the earthquake epicenters, and they act as a guide in describing and determining the potential sources and in estimating the risk presented. Therefore, it is necessary to consider the uncertainty in these parameters in the various stages of such studies. Studies conducted by Mirzaei et al. (1997) have determined a minimum error of 30 km for the epicenters of historical earthquakes, but for some of them the error increase up to 200 km. For instrumental earthquakes recorded by international authorities such as ISC, NEIC, USGS, which are the most reliable centres for determining the parameters of earthquakes, the error rate for earthquakes with

Msgreater than 6, is 10 km, and for earthquakes with Ms between 5 and 6, is 15 km (Mirzaei et al. 1997).
Regarding the uncertainty earthquake magnitude, it should be noted that the formulas used to determine magnitude are experimentally simplified by the complex processes that take place in obtaining the source of earthquake. In the studies presented by Kasahara and Narita (1985) it has been found that determining magnitude even under the best conditions is subject to an error of 0.2 to 0.3. Studies by Mirzaei et al. (1997) show that the uncertainty for historical earthquakes varies from 0.4 to 0.5.
The considerable uncertainties of historical data have a significant role in determining seismic parameters. Table 1 summarizes estimates of the existing uncertainties in determining the locations of earthquake epicenters based on magnitude and time of occurrence. This table is based on documentary reports such as those presented by Berberian (1994) and Berberian and Yeats (1999).

Table 1. Uncertainty in determining the locations of earthquake epicenters (in kilometers).

Period	Mw				
	3-4	4-5	5-6	6-7	7<
Before 1800	-	-	75-50	55-35	50-30
1800-1918	-	70-50	50-30	45-25	40-20
1918-1964	-	-	-	18	12
1964-1980	-	9.5	6.5	5.4	5.5
After 1980	13.5	8.5	4	4	3.5

It should be emphasized that the uncertainties in recorded magnitudes are not the same for historical data and instrumental data. For historical data the uncertainty can be considered equal to 0.5 large units, whereas for instrumental data before 1964 it is equal to 0.3, and for instrumental data after 1964 it is usually 0.1.

Evaluation of the completeness of the catalog

After aggregating historical and instrumental information, the reliability and completeness of the catalog must be evaluated. Due to the lack of reporting of small earthquakes in historical sources and in the early periods of instrumental data, the seismic catalog for a region is always incomplete. Because the existing catalog covers a long period of time, it contains temporal and spatial heterogeneities. The step method is used to calculate the completeness of the catalog. In this method, it is assumed that the frequency of earthquake events in a given period of time is stable and that the rate of events is constant over a large time interval with in the period:

$n = N / \Delta N$

where n is the average rate of events and N is the cumulative number of events over a large period of time.

The completeness of the data is very important for determining the seismic parameters, especially the value of b in the Gutenberg-Richter relationship (1954), which can cause errors in estimating these parameters if it is not correct. If the value of b is not specified, it is usually taken to be less than actually is. If the earthquake catalog is incomplete, it means that all events do not record their continuous occurrence in terms of magnitude and location. When drawing the Gutenberg-Richter relationship, it is observed that above a certain magnitude, the data do not follow a linear pattern, which indicates incomplete magnitude data in the data set. This is especially true for older catalog entries when recording stations were scarce and incomplete reports were submitted, and this magnitude level is set as a threshold for reliable data. Figure 4 shows the Gutenberg-Richter relationship and how Mc is determined. Finally, all earthquakes with lower magnitude values were removed for various time periods and excluded from the calculation of seismic parameters. The value of Mc in this study is 4.3 and the Gutenberg-Richter logarithmic linear equation can be calculated after allowing for imperfect magnitude.

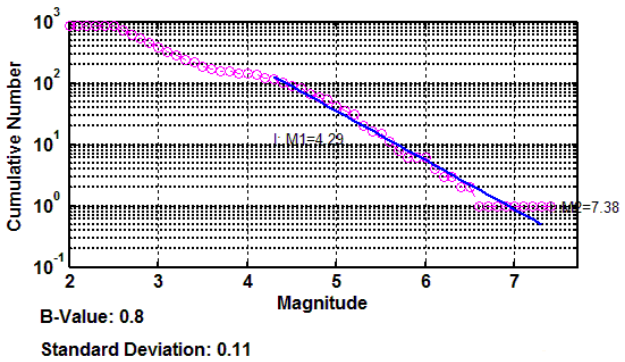

Fig 4. Calculation of magnitude and determination of seismic parameters based on Gutenberg-Richter method.

Kijko method

The catalog of seismic events in the study area consists of three sections. The first part deals with historical earthquakes that have occurred over a period of more than a few hundred years. The second part deals with systemic earthquakes from 1900 onwards. The third section includes time intervals when sufficient data are not available. Kijko and Sellevoll (1992) estimated seismic parameters using different sections of the catalog. The advantages of this method are: 1) Using dual-exponential functions 2) Using historical earthquakes together with instrumental earthquakes in estimating seismic parameters, and 3) Eliminating a large error by excluding the failure to record earthquakes during specified intervals in incomplete earthquake event lists.

The method proposed by Kijko and Sellevoll (1992) is useful because it is capable of using a list of mixed and heterogeneous earthquakes and is suitable for the characteristics of Iranian seismic data. Functions used in the Kijko program include the fitting-out distribution function for pre-twentieth-century earthquakes, which were often large but have high data errors, and the Gutenberg-Richter double-distribution function for recorded device earthquakes, which applies a statistical method to drive the maximum likelihood estimate. In this method, there are also functions that can be simultaneously applied to historical and recorded device earthquakes by performing calculations appropriate to each classification and taking into account large errors, threshold magnitudes and maximum magnitudes as required for each category. It is also possible to incorporate the effects of seismic absences or lack of information in the calculations (Kijko 1988, 2000, 2004). Estimated seismic parameters, including maximum seismic magnitude (Mmax), β coefficient and annual slope λ in a range of 100 km, using the Kijko method are: Mmax = 7.6, β = 1.7, λ = 0.98

The probability of an event with the return period of earthquakes is another case that is calculated by this software. As can be seen in Figure 5, the return period increases with a large increase and the probability of an earthquake event decreases in a certain period of time. For example, in a period of 100 years, the probability of an earthquake with a magnitude of 5.3 is 100%.

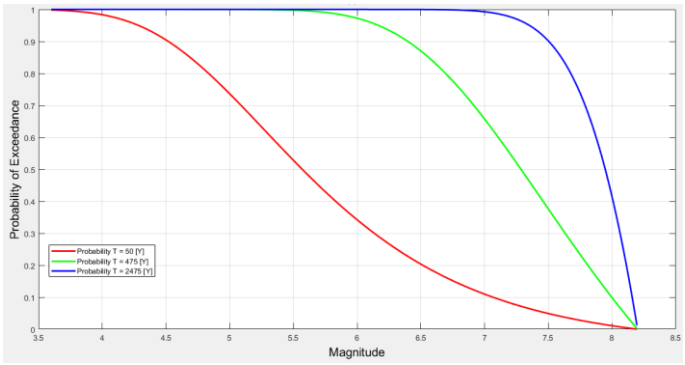

Fig 5. Re-occurrence period diagram of the study area.

Reduction relations

In seismic hazard analysis studies, the choice of reduction relations should be in accordance with the seismic-structural characteristics of the study area. If there is no accelerometric data for the study area, reduction relations can be used that closely match the seismic-tectonic conditions for the area. In order to estimate the maximum possible acceleration in the Ez-Frisk software, the following reduction relations in the horizontal component were selected: Boore-Joyner-Fumal (1997); Somerville (2000) USGS 2002; Atkinson-Boore (2006) NGA; Abrahamson-Silva (2008) NGA; Boore-Atkinson (2008) NGA; Campbell-Bozorgnia (2008) NGA.

Earthquake potential source

Seismic sources are areas that differ from neighbouring areas in terms of seismicity. The seismic pattern and the mechanism of faults play a very important role in determining these sources. In this study, the seismic sources are identified as an area that can cover the entire imaged area of the fault. In this research, 14 linear sources and 16 zone sources have been identified (Fig 6). The linear sources of the region include: Naramiq, Bozqush, Khanivardi, Yamchi, Atashgah, east of Luleh-e-Chachal, Astara, Shafarood, Bakler, Rudbar, the west of Talesh, Sangavard, Rudbar, Manjil.

Maximum magnitude

One of the most basic parameters influencing the estimation of earth movement parameters is the magnitude of earthquakes. After identifying the seismic sources, the maximum magnitude was estimated for each of these sources. Given the relationship between the magnitude of earthquakes and rupture parameters such as the amount of fault displacement (Wells and Coppersmith 1994), the maximum magnitude of earthquakes for seismic sources can be estimated using experimental relationships between magnitude and fault

length. In this study, the maximum magnitude considered for each seismic source, the mean magnitude determined in the experimental relations of Nowroozi (1985), Wells and Coppersmith (1994), Ambraseys and Jackson (1998), and Ghasemi (2014) and the maximum observational magnitude are all considered to have the same coefficients (it should be noted that in cases where the average magnitude is less than the observational magnitude, the observational magnitude is considered as the maximum magnitude). Table 2 shows the magnitude calculated for the experimental relationships used in this study. Table 3 also shows the seismic parameters used for linear and area sources in the study area.

Horizontal acceleration of seismic sources *in the study area*

In this study, the maximum acceleration due to ground motion (PGA) in different return periods is estimated. In order to investigate changes in the acceleration parameter, seismic hazard maps for PGA on bedrock have been prepared with 1% attenuation in Khalkhal city for return periods of 50 years (Fig 7) and 475 years (Fig 8), drawn at intervals of 0.1° × 0.1° in the set of networked points.

4. Discussion

In the past few decades, numerous studies on the modification of seismic ground motion by surface geology and subsurface structures (Effects of Surface Geology on seismic motion, ESG) have been carried out for improving both our understanding of strong ground motion characteristics during destructive earthquakes and our ability to perform reliable ground motion predictions of future events (Wen et al. 2018). Ground motion is a phenomenon resulting fault rupture by earthquake that damages man-made structures.

For the purpose of seismotectonic studies, the probability of fault activities of the Khalkhal area carried out in this research. The maximum magnitude and ground-motion were determined and predicted. There is no damaged event in the Khalkhal region by now. Some factors influenced the magnitude of earthquake such as: rate of stress, differential stresses, rock mechanics (elasticity and Poisson's modulus) and dimension of fault. The long faults, make the large shakes in ground. Landslide, exhumation, subsidence, long length fractures, springs, tsunami and liquefaction are the evidence of an earthquake. The historical events help for the estimation of earthquake hazards in the future. According to the model of Rezaeian et al. (2020), layered units in the Khalkhal region had a NW-SE strike in the Oligocene. Since then the strike has been rotated clockwise so that now it is almost N-S. Field investigations and paleostress studies Sadeghi et al. (2015) indicate that the clockwise rotation has been brought about movement on two main sinistral strike-slip faults, in response to the continuing Arabia-Eurasia collision.

Similarly, in the western part of the Alborz Mountains, sinistral strike-slip faults and a fold-and-thrust system continues to accommodate Arabia-Eurasia convergence, with a total shortening of 15-18 km since the Late Miocene (Guest et al. 2006). The overall tectonic regime in the region is compressive, with the dominant compressive forces causing the rotation of linear structural trends.

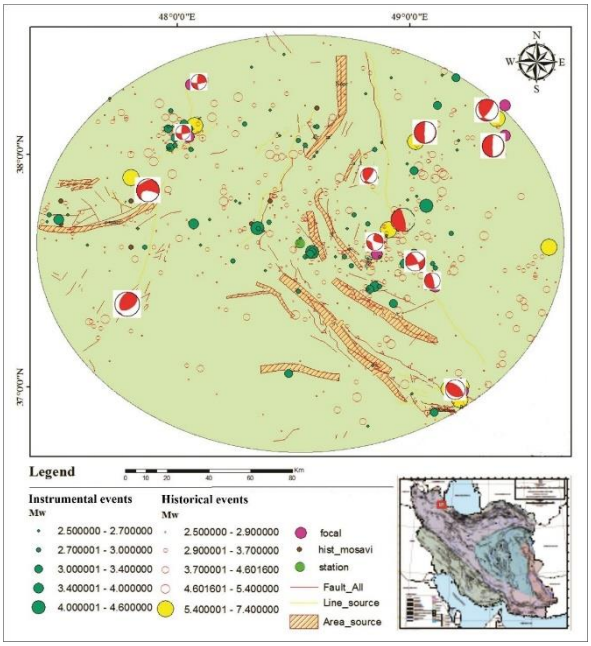

Fig 6. Seismotectonic map (zonal and linear sources determined along with the focal mechanism of earthquakes surveyed within a radius of 100 km of Khalkhal city).

Table 2. Calculation of maximum magnitude for seismic sources in this study

No	Fault Zone		Fault Length	Observed Mmax	Rupture (Km)	Nowroozi (1985)	Wells and CopperSmith (1994)	Ambraseys and Jackson (1998)	Ghasemi (2014)	Mean Empirical (Mmax)	Final Mmax*
1	Line Source	Narmiq	8.84	7.4	4.42	5.8	5.8	5.9	6.1	5.9	7.4
2		Bozqush	32.18	6.7	16.09	6.5	6.5	6.5	6.6	6.5	6.7
3		Khanyordi	11.77	6.8	5.885	5.9	6.0	6.0	6.2	6.0	6.8
4		Yamchi	18.51	6.7	9.255	6.2	6.2	6.2	6.4	6.2	6.7
5		Atashgah	12.59	7.1	6.295	6.0	6.0	6.0	6.2	6.1	7.1
6		East of Lulehchal	13.8	6.8	6.9	6.0	6.1	6.1	6.3	6.1	6.8
7		Astara	103	6.9	51.5	7.1	7.1	7.1	7.0	7.1	7.1
8		Shafarud	6.45	7.3	3.225	5.6	5.7	5.7	6.0	5.7	7.3
9		Baklor	24.72	6.9	12.36	6.3	6.3	6.4	6.5	6.4	6.9
10		Rudbar	20.58	7.1	10.29	6.3	6.3	6.3	6.4	6.3	7.1
40		West of Talesh	16.66	7.0	8.33	6.1	6.1	6.2	6.3	6.2	7.0
41		Sangavard	45.87	7.0	22.935	6.7	6.7	6.7	6.7	6.7	7.0
42		Rudbar	6.27	6.7	3.135	5.6	5.7	5.7	6.0	5.7	6.7
43		Manjil	52.6	6.6	26.3	6.8	6.7	6.7	6.8	6.7	6.7
44	Area Source	Giljin	50.8	6.8	25.4	6.7	6.7	6.7	6.7	6.7	6.8
45		Dordelvar	68.5	7.0	34.25	6.9	6.9	6.9	6.9	6.9	7.0
46		Jeraz	92	6.9	46	3.4	23.0	1.7	11.5	0.9	5.8
47		Qarpuzlu	89.2	7.0	44.6	3.5	22.3	1.8	11.2	0.9	5.6
48		Noor	49	7.1	24.5	3.6	12.3	1.8	6.1	0.9	3.1
49		Andalibi	36.3	7.1	18.15	3.5	9.1	1.8	4.5	0.9	2.3
50		Delmadeh	63.2	6.8	31.6	3.4	15.8	1.7	7.9	0.9	4.0
51		Masuleh	77.3	6.9	38.65	3.4	19.3	1.7	9.7	0.9	4.8
52		Vanno	68.5	7.0	34.25	3.5	17.1	1.8	8.6	0.9	4.3
53		Andarab	91.5	7.0	45.75	3.5	22.9	1.8	11.4	0.9	5.7
54		Doniq	114.6	6.8	57.3	3.4	28.7	1.7	14.3	0.8	7.2
55		Benarvan	105.6	6.7	52.8	3.4	26.4	1.7	13.2	0.8	6.6
56		West of Lulehchal	50.8	6.8	25.4	3.4	12.7	1.7	6.4	0.9	3.2
57		Ardeh	68.5	6.9	34.25	3.5	17.1	1.7	8.6	0.9	4.3
58		Niki	92	6.9	46	3.4	23.0	1.7	11.5	0.9	5.8
59		Kellass	89.2	7.0	44.6	3.5	22.3	1.8	11.2	0.9	5.6

Table 3. Seismicity parameters used for linear and zonal sources in the study area

Seismic Source Name		Det. Mag.	Seismogenic Depth	Dip	Min. Mag.	Beta	Activity Rate	Fault Length
Line Source	Narmiq	7.4	5 to 30	5	4.3	1.27	0.009199013	56.5
	Bozqush	6.731	5 to 30	45	4.3	1.27	0.033486905	18.95
	Khanyordi	6.762	5 to 30	45	4.3	1.27	0.012248007	29.03
	Yamchi	6.652	5 to 30	70	4.3	1.27	0.019261735	31.69
	Atashgah	7.094	5 to 30	70	4.3	1.27	0.013101309	48.38

Table 3. Continued.

Seismic Source Name		Det. Mag.	Seismogenic Depth	Dip	Min. Mag.	Beta	Activity Rate	Fault Length
Line Source	East of Lulehchal	6.755	5 to 30	90	4.3	1.27	0.01436045	22.01
	Astara	7.069	5 to 30	45	4.3	1.27	0.107183072	51.3
	Shafarud	7.298	5 to 30	45	4.3	1.27	0.00671195	32.97
	Baklor	6.947	5 to 30	53	4.3	1.27	0.025723937	54.7
	Rudbar	7.090	5 to 30	61	4.3	1.27	0.021415802	165.8
	west of Talesh	7.015	5 to 30	45	4.3	1.27	0.017336602	50.8
	Sangavard	7.001	5 to 30	45	4.3	1.27	0.047732888	68.5
	Rudbar	6.713	5 to 30	45	4.3	1.27	0.006524639	92
	Manjil	6.747	5 to 30	35	4.3	1.27	0.05473621	89.2
Area Source	Giljin	6.835	5 to 30	-	4.3	1.27	0.052863107	49
	Dordelvar	6.972	5 to 30	-	4.3	1.27	0.071281946	36.3
	Jeraz	5.75	5 to 30	-	4.3	1.27	0.095736336	63.2
	Qarpuzlu	5.575	5 to 30	-	4.3	1.27	0.092822621	77.3
	Noor	3.0625	5 to 30	-	4.3	1.27	0.050990005	68.5
	Andalibi	2.268	5 to 30	-	4.3	1.27	0.037774228	91.5
	Delmadeh	3.95	5 to 30	-	4.3	1.27	0.0657667	114.6
	Masuleh	4.831	5 to 30	-	4.3	1.27	0.080439335	105.6
	Vanno	4.281	5 to 30	-	4.3	1.27	0.071281946	50.8
	Andarab	5.718	5 to 30	-	4.3	1.27	0.09521603	68.5
	Doniq	7.162	5 to 30	-	4.3	1.27	0.119254175	92
	Benarvan	6.6	5 to 30	-	4.3	1.27	0.109888664	89.2
	west of lulehchal	3.175	5 to 30	-	4.3	1.27	0.052863107	49
	Ardeh	4.281	5 to 30	-	4.3	1.27	0.071281946	36.3
	Niki	5.75	5 to 30	-	4.3	1.27	0.095736336	63.2
	Kellass	5.575	5 to 30	-	4.3	1.27	0.092822621	77.3

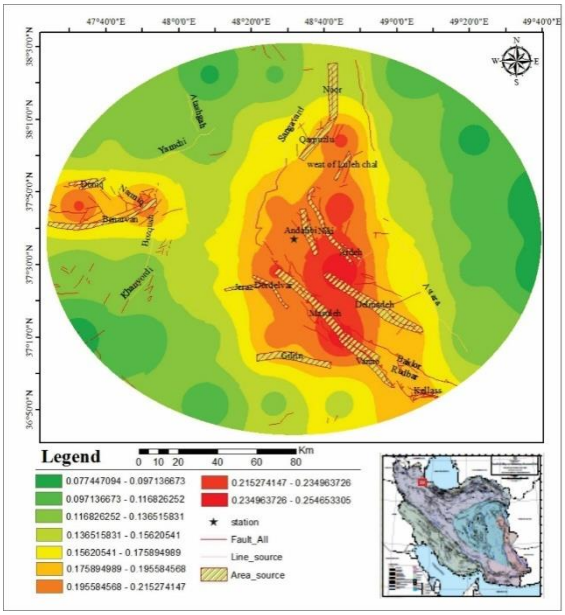

Fig 7. Horizontal component acceleration zonation map for a return period of 50 years.

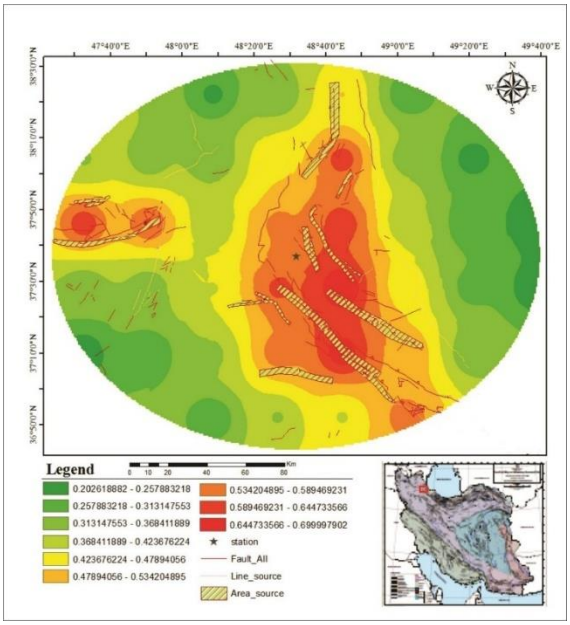

Fig 8. Horizontal component acceleration zonation map for a return period of 475 years.

5.Conclusion

In this research, 14 linear sources and 16 wide sources have been identified. From the results of the software analysis of focal mechanisms and the seismic power of faults, it has been determined that the main changes and instability in the region are due to changes in the trends of N-S and NE-SW faults. There are among the main faults in the region and have been observed in outcrop. The tectonic stresses responsible for this tectonic activity have been in place since the end of the Cretaceous and replaced earlier stress regimes existing in and before Cretaceous times.

The occurrence of small earthquakes (less than 3 on the Richter scale) indicates that the region continues to be tectonically active and that energy continues to be released by movement on active faults. The return periods of 50 years and 475 years illustrate on the probability of earthquakes with magnitudes above 5.3 on the Richter scale is definitive within the 100 years in mean.

Acknowledgments

The authors thank Urmia University for support and Professor Peter Colman for valuable and constructive comments on the manuscript.

Conflict of interest

The authors declare that they have no conflict of interest and also have no known competing financial interests or personal relationships that could have appeared to influence the work reported in this paper.

References

Abrahamson NA, Silva WJ (2008) Summary of the Abrahamson and Silva NGA ground-motion relations. *Earthquake Spectra* 24 (1): 67-97.

Ambraseys NN, Jackson JA (1998) Faulting associated with historical and recent earthquakes in the Eastern Mediterranean region. *Geophysical Journal International* 133: 390-406.

Ambraseys NN, Melville CP (1982) A history of Persian earthquakes. Cambridge University Press, Cambridge, Britain.

Asadian O, Mirzaei AR, Eftekharnezhad J, Ghomashi A, Nozari A (1999) Geological map of Khalkhal-Rezwanshahr quadrangle. Geological Survey of Iran. Quadrangle map scale, 1/100000.

Atkinson GM, Boore DM (2006) Earthquake Ground-Motion Prediction Equations for Eastern North America. *Bulletin of the Seismological Society of America96 (6): 2181-2205*.

Berberian M (1994) Natural hazards and the first earthquake catalogue of Iran. International Institute of Earthquake Engineering and Seismology (IIEES). Tehran, Iran: 1, 620.

Berberian M, Yeats RS (1999) Patterns of historical earthquake rupture in the Iranian plateau. *Bulletin of the Seismological Society of America* 89 (1): 120-139.

Boore DM, Joyner WB, Fumal TE (1997) Equations for Estimating Horizontal Response Spectra and Peak Acceleration from Western North American Earthquakes: A Summary of Recent Work. *Seismological Research Letters* 68 (1): 128-153.

Boore DM, Atkinson GM (2008) Ground-motion prediction equations for the average horizontal component of PGA, PGV, and 5%-damped PSA at spectral periods between 0.01 s and 10.0 s. *Earthquake Spectra* 24 (1): 99-138.

Campbell KW (1997) Empirical near-source attenuation relationships for horizontal and vertical components of peak ground acceleration, peak ground velocity, and

pseudo-absolute acceleration response spectra. *Seismological Research Letters* 68 (1): 154-179.

Campbell KW, Bozorgnia Y (2008) NGA ground motion model for the geometric mean horizontal component of PGA, PGV, PGD and 5% damped linear elastic response spectra for periods ranging from 0.01 to 10 s. *Earthquake Spectra* 24 (1): 139-171.

Darvishzadeh A (2006) Geology of Iran (Stratigraphy, Tectonic, Metamorphism and Magmatism). *Amirkabir Publications* 30(1):23-7.

Dehghan AN, Yazdi A (2023) A Geomechanical Investigation for Optimizing the Ultimate Slope Design of Shadan Open Pit Mine, Iran, *Indian Geotechnical Journal*, 1-15.

Doroozi R, Vaccaro C, Masoudi F, Petrini R (2016) Cretaceous alkaline volcanism in south Marzanabad, northern central Alborz, Iran: Geochemistry and petrogenesis Geoscience. *Frontiers* 7: 937-95.

Gardner JK, Knopoff L (1974) Is the sequence of earthquake in southern California, with aftershocks removed, Poissonian*? Bulletin of the Seismological Society of America* 64 (5): 1363-1367.

Ghasemi MR (2016) Surface ruptures of the Iranian earthquakes 1900-2014: Insights for earthquake fault rupture hazards and empirical relationships. *Earth-Science Reviews* 156: 1-13.

Guest B, Axen GJ, Lam, PS, Hassanzadeh J (2006) Late Cenozoic shortening in the westcentralAlborz Mountains, northern Iran, by combined conjugate strike-slip and thin-skinned deformation. *Geosphere* 2: 35-52.

Gutenberg B, Richter CF (1944) Frequency of earthquakes in California. *Bulletin of the Seismological Society of America* 34(4): 185-188.

Gutenberg B, Richter CF (1954) Seismicity of the earth and associated phenomena. Princeton University Press, New Jersey.

Karimiazar J, SharifiTeshnizi E, O'Kelly BC, SadeghiSh, Karimizad N, Yazdi A, Arjmandzadeh R (2023) Effect of Nano-Silica on Engineering Properties of Lime-Treated Marl Soil, *Transportation Geotechnics* 43, 101123

Kasahara H, Narita S (1985) Practical multiprocessor scheduling algorithms for efficient parallel processing. *Systems and computers in Japan* 16: 11-16.

Kijko A (1988) Maximum likelihood estimation of Gutenberg-Richter b parameter for uncertain magnitudes values. *Pure and Applied geophysics* 127: 573-579.

Kijko A (2000) Statistical estimation of maximum regional earthquake magnitude Mmax, Workshop of Seismicity Modeling in Seismic Hazard Mapping, Poljce, Slovenia. *Geol Survey May* 22-24, 1-10.

Kijko A (2004) Estimation of the maximum earthquake magnitude, Mmax. *Pure Applied Geophysics* 161(8): 1655–1681.

Kijko A, Sellevoll MA (1992) Estimation of earthquake hazard parameters from incomplete data files. Part Π. Incorporation of magnitude hetregenity. *Bulletin of the Seismological Society of America* 82: 120-134.

Madanipour S, Yassaghi A, Ehlers TA, Enkelmann E (2018) Tectonostratigraphy, structural geometry and kinematics of the NW Iranian Plateau margin: Insights from the Talesh Mountains, Iran. *American Journal of Science* 318 (2): 208-245.

Mirzaei N, Gao M, Chen YT (1997) Evaluation of uncertainty of earthquakes parameters for the purpose of seismic zoning of Iran. Earthquake Research in *China* 11: 197-212.

Nazari H, Shahidi A (2011) Tectonic of Iran «Alborz». Geological Survey and Mineral Exploration of Iran. Research Institute for Earth Science, 97p.

Nowroozi A (1985) Empirical relations between magnitude and fault parameters for earthquakes in Iran. *Bulletin of the Seismological Society of America* 75 (5): 1327-1338.

Reasenberg P (1985) Second-order moment of central California seismicity, 1969-1982. *Journal of Geophysical Research: Solid Earth* 90 (B7): 5479-5495.

Rezaeian M, Kuijper CB, van der Boon A, Pastor-Gálan D, Cotton LJ, Langereis CG, Krijgsman W (2020) Post-Eocene coupled oroclines in the Talesh (NW Iran). Paleomagnetic constraints. *Tectonophysics* 786: 228-459.

Sadeghi R, Saeedi A, Arian M, Ghorashi M, Solgi A (2015) Comparison of Strain Ellipsoid Shape in the South of Ardabil Range (NW), Based on the Results of the Magnetic Susceptibility Anisotropy and Paleostress Methods. *Open Journal of Geology* 5: 611-622.

Somerville PG (2000) Magnitude scaling of near fault ground motion. Proc. Int. *Workshop on Annual Commemoration of Chi-Chi earthquake 1, 59-70*.

VahdatiDaneshmand F, Nadim H (2001) Geological map of Marzanabad quadrangle. Geological Survey of Iran. Quadrangle map scale, 1/100000.

Wells DL, Coppersmith KJ (1994) New Empirical Relationships among Magnitude, Rupture Length, Rupture Width, Rupture Area and Surface Displacement. *Bulletin of the Seismological Society of America* 84 (4): 974-1002.

Wen KL, Bard PY, Sánchez-Sesma FJ, Higashi S, Iwata T, Maeda T (2018) Effect of surface geology on seismic motion: challenges of applying ground motion simulation to seismology and earthquake engineering. Earth, *Planets and Space* 70: 178.

Zhuang J, Ogata Y, Vere-Jones D (2002) Stochastic declustering of space-time earthquake Occurrences. *Journal of the American Statistical Association* 97 (458): 369-380.